



Dynamic modeling and stability analysis of power networks using $dq0$ transformations with a unified reference frame

Juri Belikov^{a*} and Yoash Levron^b

^a Department of Computer Systems, Tallinn University of Technology, Akadeemia tee 15a, 12616 Tallinn, Estonia

^b The Andrew and Erna Viterbi Faculty of Electrical Engineering, Technion—Israel Institute of Technology, Haifa 3200003, Israel

Received 21 February 2018, accepted 15 May 2018, available online 23 October 2018

© 2018 Authors. This is an Open Access article distributed under the terms and conditions of the Creative Commons Attribution-NonCommercial 4.0 International License (<http://creativecommons.org/licenses/by-nc/4.0/>).

Abstract. The $dq0$ reference frame has become popular for modeling and control of traditional electric machines and small power sources. However, its widespread use for modeling and analysis of large-scale, general power systems is still a pending issue. One problem that arises when considering $dq0$ models is that they are typically based on local reference frames, and therefore linking different models is not straightforward. In this paper we propose to approach this problem by modeling the network and its components using a $dq0$ transformation that is based on a unified reference frame. We demonstrate this idea on the basis of synchronous machines and photovoltaic generators, and we also establish a $dq0$ -based dynamic model of a transmission network. The resulting models all use a unified reference frame, and therefore can be directly linked to each other in simulation and analytically. The paper is accompanied by a free software package (Levron, Y. and Belikov, J. Toolbox for Modeling and Analysis of Power Networks in the DQ0 Reference Frame. 2016. www.mathworks.com/matlabcentral/fileexchange/58702) that constructs the proposed dynamic models and provides tools for dynamic simulations and stability studies based on $dq0$ quantities.

Key words: power systems, $dq0$ transformation, renewable energy, stability.

1. INTRODUCTION

In recent years, the increasing penetration of small distributed generators and fast power electronics based devices has given rise to new challenges in modeling the dynamics of power systems. This becomes evident when considering large-scale systems for which it is especially important to maintain the balance between accuracy and complexity. This challenge has led to new dynamic models of power systems that are based on direct-quadrature-zero ($dq0$) quantities [1]. Such models are not as general as three-phase (abc)-based (EMTP-like) models and are advantageous mainly when the transmission network and units are balanced. However, $dq0$ models combine two properties of interest: similar to transient models, $dq0$ models are derived from physical representations, and are therefore accurate at high frequencies, and as a result the assumption of slowly varying signals is not re-

quired. In addition, $dq0$ models are time-invariant, which allows defining an operating point, and enables small-signal analysis. A detailed comparison of simulation techniques based on the abc and $dq0$ reference frames can be found in [2,3].

The $dq0$ transformation has been traditionally used in transient analysis of electric machines [4] and is increasingly used today for modeling distributed sources, complex loads, renewable generators, and on devices based on power electronics [5–7]. However, widespread use of this transformation for modeling large-scale power systems is still a pending issue. Toward this end, one problem that arises when considering $dq0$ models is that units are typically based on local reference frames, and therefore linking different models is not straightforward. The idea of modeling a transmission network and loads in a common dq reference frame was presented in [1,8], assuming that the network consists only of resistors and

* Corresponding author, juri.belikov@ttu.ee

inductors. These works consider a common reference frame, meaning that all the units and the network share the same reference, see [9]. Work [10] presents $dq0$ -based models of three-phase networks with RL elements. Work [11] develops a small-signal $dq0$ model of a microgrid that includes synchronous machines and electronically interfaced distributed generators. In addition, an attempt to derive a model of a general network is presented in [12], where it is shown how to construct a state-space model of the network that is nonminimal. A further extension of this paper is presented in [13].

In this paper we continue these ideas and propose a method for modeling the network and its components using a $dq0$ transformation that is based on a unified reference frame, where the main objective is to create $dq0$ -based models of large-scale power systems that are both accurate and time-invariant. The resulting models all use a unified reference frame, and therefore can be directly linked to each other in simulation and analytically. We open the paper by recalling the basic transformation from one reference frame to another and demonstrate this process using the classic example of a synchronous machine connected to an infinite bus. The paper then extends this example and presents a $dq0$ -based dynamic model of a general transmission network, using ideas presented in [10,14] and based on the network topology defined in MATPOWER [15]. We also develop models of several typical units. This approach is demonstrated numerically in a dedicated software tool available in [16]. Several numeric examples are described in detail: a 4-bus system showing comparison between quasi-static, abc -, and $dq0$ -models; a 14-bus system illustrating the joint dynamics of synchronous machines, photovoltaic generators, and the transmission network; and a large 200-bus system demonstrating small-signal analysis.

2. PRELIMINARIES AND A MOTIVATING EXAMPLE

Consider a reference frame rotating with an angle of $\theta(t)$. For instance, in a synchronous machine, $\theta(t)$ is typically selected to be the rotor electrical angle. Let $\tilde{\zeta}$ represent the quantity to be transformed (current, voltage, or flux), and use the compact notation $\zeta_{abc} = [\zeta_a, \zeta_b, \zeta_c]^T$, $\zeta_{dq0} = [\zeta_d, \zeta_q, \zeta_0]^T$. Then, the $dq0$ transformation can be written as [4, Appendix C]

$$\tilde{\zeta}_{dq0} = T_\theta \zeta_{abc} \quad (1)$$

with

$$T_\theta = \frac{2}{3} \begin{bmatrix} \cos(\theta) & \cos(\theta - \frac{2\pi}{3}) & \cos(\theta + \frac{2\pi}{3}) \\ -\sin(\theta) & -\sin(\theta - \frac{2\pi}{3}) & -\sin(\theta + \frac{2\pi}{3}) \\ \frac{1}{2} & \frac{1}{2} & \frac{1}{2} \end{bmatrix}.$$

Further in this paper we aim to explore an alternative reference frame that rotates with the unified angle $\omega_s t$,

where ω_s is the steady-state system frequency or the frequency of an infinite bus, see [17] for more details. We will show that such selection provides several advantages in the connectivity of a large variety of system components and also can be used to derive compact and easy-to-use small-signal models describing the power system dynamics. The $dq0$ transformation can be redefined with respect to a new reference frame rotating with an angle $\omega_s t$ by direct substitution of $\theta = \omega_s t$ in (1) as

$$\zeta_{dq0} = T_{\omega_s} \zeta_{abc}. \quad (2)$$

A formula that allows conversion of signals from the standard reference frame (defined with respect to θ) to the new frame (defined with respect to $\omega_s t$) is given as

$$\begin{bmatrix} \zeta_d \\ \zeta_q \\ \zeta_0 \end{bmatrix} = \begin{bmatrix} \sin(\delta) & \cos(\delta) & 0 \\ -\cos(\delta) & \sin(\delta) & 0 \\ 0 & 0 & 1 \end{bmatrix} \begin{bmatrix} \tilde{\zeta}_d \\ \tilde{\zeta}_q \\ \tilde{\zeta}_0 \end{bmatrix}, \quad (3)$$

where $\delta(t) = \theta(t) - \omega_s t + \pi/2$, the variables $\tilde{\zeta}_d$, $\tilde{\zeta}_q$ are defined with respect to θ , and ζ_d , ζ_q are defined with respect to $\omega_s t$.

To explain the idea of a unified reference frame, we start by recalling a classical model of a synchronous machine connected to an infinite bus, and present both models using a unified reference frame. Assume a simplified synchronous machine represented as an ideal voltage source behind a synchronous inductance \tilde{L}_d . The machine is connected to an infinite bus, as shown in Fig. 1. Both the infinite bus and the internal synchronous machine are represented as voltage sources. The synchronous machine voltage is $\tilde{v}_d = 0$, $\tilde{v}_q = V_e$, $v_0 = 0$, with a reference angle of θ . In this example θ is the electric angle of the rotor in respect to the stator. The infinite bus has a constant frequency of ω_s , so its voltage is given by $v_d = V_g$, $v_q = 0$, $v_0 = 0$, with a reference angle of $\omega_s t$.

Now the goal is to construct a dynamic model of the complete system based on $dq0$ signals. However, a potential problem is that the two voltage sources are defined with respect to two different reference frames (θ and $\omega_s t$). To solve this, we choose $\omega_s t$ as a unified reference frame for both the infinite bus and synchronous machine, and construct a model of the synchronous machine

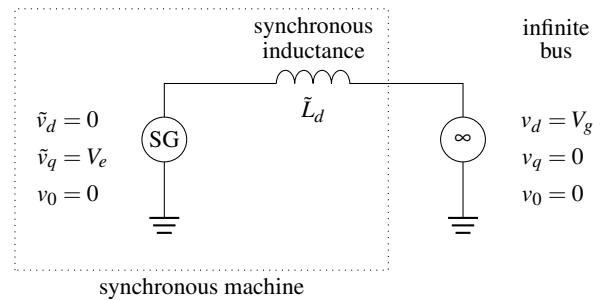


Fig. 1. Single-phase diagram of a simple synchronous machine (SG) connected to an infinite bus (∞).

using signals in this reference frame. The synchronous machine voltage is now obtained by substituting $\tilde{v}_d = 0$, $\tilde{v}_q = V_e$, $v_0 = 0$ in (3), which yields

$$\begin{bmatrix} v_d \\ v_q \\ v_0 \end{bmatrix} = \begin{bmatrix} V_e \cos(\delta) \\ V_e \sin(\delta) \\ 0 \end{bmatrix}, \quad (4)$$

$$\delta = \theta - \omega_s t + \pi/2.$$

In addition, the dynamic behavior of the angle δ is described by

$$\frac{d^2}{dt^2} \delta = \frac{\text{poles}}{2J\omega_s} \left(-P_{3\phi} + P_m - K_d \frac{d}{dt} \delta \right), \quad (5)$$

which is the classic *swing equation*. The term J is the rotor constant of inertia, *poles* is the number of machine poles (must be even), P_m is the mechanical power, and K_d is the damping constant. The three-phase power can be computed as $P_{3\phi} = \frac{3}{2}(v_d i_d + v_q i_q + 2v_0 i_0)$. Let $\delta = \phi_1$, then the combination of (4) and (5) results in a state-space model given as

$$\begin{aligned} \frac{d}{dt} \phi_1 &= \phi_2, \\ \frac{d}{dt} \phi_2 &= \frac{\text{poles}}{2J\omega_s} \left(-\frac{3}{2} V_e (\cos(\phi_1) i_d + \sin(\phi_1) i_q) \right. \\ &\quad \left. + P_m - K_d \phi_2 \right), \\ v_d &= V_e \cos(\phi_1), \quad v_q = V_e \sin(\phi_1), \quad v_0 = 0. \end{aligned} \quad (6)$$

Note that the model represents only the machine's voltage source and does not include the synchronous inductance, which is modeled separately in the next section.

3. MODELING POWER SYSTEM COMPONENTS USING A UNIFIED REFERENCE FRAME

In this section we show that this idea can be extended and that complex networks and various power system units can be connected to each other by using signals that are defined with respect to the unified reference frame. This allows us to obtain a complete model of the system that is based entirely on $dq0$ quantities, and thus provides a constructive method to analyze the system's dynamic behavior.

3.1. State-space models of linear passive transmission networks

We open this section by developing models of single passive components [18], using the unified reference frame. The discussion that follows shows how to combine these models to describe the dynamics of general transmission

networks. The dynamic model of an inductor is given in the abc reference frame as

$$L \frac{d}{dt} I_{abc,12} = V_{abc,1} - V_{abc,2}, \quad (7)$$

and can be converted to the $dq0$ frame as follows. Observe that the differentiation of T_{ω_s} results in

$$\frac{d}{dt} I_{dq0} = \frac{dT_{\omega_s}}{dt} I_{abc} + T_{\omega_s} \frac{d}{dt} I_{abc}, \quad (8)$$

and the derivative of T_{ω_s} can be expressed as

$$\frac{d}{dt} T_{\omega_s} = \begin{bmatrix} 0 & \omega_s & 0 \\ -\omega_s & 0 & 0 \\ 0 & 0 & 0 \end{bmatrix} T_{\omega_s} = \mathscr{W} T_{\omega_s}. \quad (9)$$

Substitute (7) and (9) into (8), and use relations (2) to get

$$\frac{d}{dt} I_{dq0,12} = \mathscr{W} I_{dq0,12} + \frac{1}{L} (V_{dq0,1} - V_{dq0,2}). \quad (10)$$

This equation describes a state-space model of the three-phase inductor. Analogously, the model of a capacitor C is given as

$$\frac{d}{dt} (V_{dq0,1} - V_{dq0,2}) = \mathscr{W} (V_{dq0,1} - V_{dq0,2}) + \frac{1}{C} I_{dq0,1}.$$

And for a resistor R the model is given by simple static relations

$$V_{dq0} = I_3 R I_{dq0}, \quad (11)$$

where I_3 denotes the 3×3 identity matrix.

Similarly, by combining elementary passive components, any balanced transmission network can be modeled based on the unified reference frame. Define the $dq0$ signals $v_{d,n}, v_{q,n}, v_{0,n}$ to be the voltages on bus n ; $i_{d,n}, i_{q,n}, i_{0,n}$ to be the injected currents to bus n ; and $V_d(t) = [v_{d,1}(t), \dots, v_{d,N}(t)]^T$, $I_d(t) = [i_{d,1}(t), \dots, i_{d,N}(t)]^T$, etc., where N is the number of buses. Assume a network with the standard branch [15] as in Fig. 2.

This network can be represented in the minimal state-space form using $dq0$ signals as [13]

$$\begin{aligned} \frac{d}{dt} \xi &= A_\xi \xi + B_\xi u, \\ y &= C_\xi \xi + D_\xi u, \end{aligned} \quad (12)$$

where $u = [V_d, V_q, V_0]^T$ and $y = [I_d, I_q, I_0]^T$.

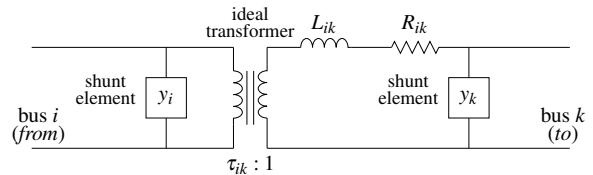


Fig. 2. Standard branch connecting buses i and k .

In addition, often disconnected buses should be eliminated. The need for this arises in several situations:

- Sometimes certain buses are not connected to either a generator or a load. In this case the current injected into the bus is zero.
- Frequently loads are modeled as shunt elements and are integrated into the network model. In this case load buses appear as disconnected buses with zero current.
- In many scenarios there is a need to analyze the dynamics or stability of a certain subset of units in the network, typically only the generators. In such cases elimination of the disconnected buses results in a simpler dynamic model in which the inputs and outputs relate only to the required subset of buses. This is usually done after integrating the loads into the network model as shunt elements.

The dynamic model after disconnected buses have been eliminated is

$$\begin{aligned} \frac{d}{dt} \tilde{\xi} &= \tilde{A}_{\tilde{\xi}} \tilde{\xi} + \tilde{B}_{\tilde{\xi}} \tilde{u}, \\ \tilde{y} &= \tilde{C}_{\tilde{\xi}} \tilde{\xi} + \tilde{D}_{\tilde{\xi}} \tilde{u}, \end{aligned} \quad (13)$$

where \tilde{u} and \tilde{y} represent the input/output following the reduction procedure. Bus elimination is achieved by controlling the inputs of the buses being eliminated, so that the corresponding outputs are zeroed. Assume for instance that the i th input and i th output are eliminated. This is done using the dynamic model output equation $y = C_{\xi} \xi + D_{\xi} u$. In case the matrix D_{ξ} of the original $dq0$ model is diagonal, the output y_i may be zeroed by controlling the i th input so that $u_i = -D_{i,i}^{-1} C_i \xi$, where C_i is the i th row in matrix C_{ξ} . Thus, the input u_i and the output y_i are eliminated and will not appear in the reduced model. In more complex systems, there is a need to transform the state vector and to compute a new dynamic model such that the corresponding rows in $\tilde{C}_{\tilde{\xi}}$ are also zero. This may be achieved by a LU decomposition of the relevant rows in C_{ξ} . More details regarding this procedure may be found in [16].

3.2. Physical synchronous machine

For completeness, consider a more sophisticated (physical) model of a synchronous machine [4]. The model presented herein captures the interaction of the direct-axis magnetic field with the quadrature-axis mmf and of the quadrature-axis magnetic field with the direct-axis mmf, as well as the effects of resistances, transformer voltages, field winding dynamics, and salient poles. The parameters are explained in Table 1.

By following [4] and omitting laborious algebraic manipulations, the resulting state-space model of a synchronous machine in the $dq0$ reference frame (with respect to $\omega_s t$) is given by

$$\begin{aligned} \frac{d}{dt} \phi_1 &= -\frac{2R_a L_{ff}}{L_{\beta}^2} \phi_1 + \phi_2 \phi_5 + \frac{2R_a L_{af}}{L_{\beta}^2} \phi_4 \\ &\quad + \sin(\phi_6) v_d - \cos(\phi_6) v_q, \\ \frac{d}{dt} \phi_2 &= -\frac{R_a}{L_q} \phi_2 - \phi_1 \phi_5 + \cos(\phi_6) v_d + \sin(\phi_6) v_q, \\ \frac{d}{dt} \phi_3 &= -\frac{R_a}{L_0} \phi_3 + v_0, \\ \frac{d}{dt} \phi_4 &= \frac{3R_f L_{af}}{L_{\beta}^2} \phi_1 - \frac{2R_f L_d}{L_{\beta}^2} \phi_4 + v_f, \\ \frac{d}{dt} \phi_5 &= \text{poles} \left(T_m + \frac{3L_{\beta}^2 - 6L_{ff} L_q}{2L_{\beta}^2 L_q} \phi_1 \phi_2 + \frac{3L_{af}}{L_{\beta}^2} \phi_2 \phi_4 \right), \\ \frac{d}{dt} \phi_6 &= \phi_5 - \omega_s \end{aligned} \quad (14)$$

with outputs defined as

$$\begin{aligned} i_d &= -\frac{2L_{ff}}{L_{\beta}^2} \sin(\phi_6) \phi_1 - \frac{1}{L_q} \cos(\phi_6) \phi_2 + \frac{2L_{af}}{L_{\beta}^2} \sin(\phi_6) \phi_4, \\ i_q &= \frac{2L_{ff}}{L_{\beta}^2} \cos(\phi_6) \phi_1 - \frac{1}{L_q} \sin(\phi_6) \phi_2 - \frac{2L_{af}}{L_{\beta}^2} \cos(\phi_6) \phi_4, \\ i_0 &= -\frac{1}{L_0} \phi_3, \quad i_f = -\frac{3L_{af}}{L_{\beta}^2} \phi_1 + \frac{2L_d}{L_{\beta}^2} \phi_4, \\ \omega &= \phi_5, \quad \delta = \phi_6, \end{aligned}$$

where $L_{\beta}^2 = 2L_d L_{ff} - 3L_{af}^2$. In this model, the state variables are $\phi_1 = \lambda_d$, $\phi_2 = \lambda_q$, $\phi_3 = \lambda_0$, $\phi_4 = \lambda_f$, $\phi_5 = \omega$, $\delta = \phi_6$; the inputs are v_d , v_q , v_0 , v_f , T_m ; and the outputs are i_d , i_q , i_0 , i_f , ω . Unlike the simplified model (6), this model includes the inductance terms L_d , L_q , L_0 .

A convenient property of the model presented above is that its inputs and outputs are defined with respect to the unified reference frame rotating with $\omega_s t$, and therefore it can be directly connected to the network. For instance, connecting the synchronous machine model to

Table 1. Nomenclature: synchronous machine

Variable	Description
$\lambda_d, \lambda_q, \lambda_0$	Flux linkages
λ_f	Field winding flux linkage
$\tilde{v}_d, \tilde{v}_q, v_0$	Stator voltages
$\tilde{i}_d, \tilde{i}_q, i_0$	Stator currents
v_f, i_f	Field windings voltage and current
L_d, L_q, L_0	Synchronous inductances
L_{af}	Mutual inductance between the field winding and phase a
L_{ff}	Self-inductance of the field winding
R_a, R_f	Armature and field winding resistance
J	Rotor moment of inertia
T_m	Mechanical torque

an infinite bus is immediate. An infinite bus with a frequency of ω_s is defined in this reference frame by $v_d = \sqrt{2}V_g$, $v_q = v_0 = 0$, where V_g is the infinite bus RMS voltage. Therefore, a synchronous machine connected to an infinite bus can be modeled by direct substitution of these voltages into (3.2).

3.3. Photovoltaic generator

Similarly to the synchronous machine, photovoltaic inverters can also be represented in the unified reference frame that rotates with $\omega_s t$. Several models of photovoltaic generators are available in the recent literature, as reviewed in [10]. Regardless of the model used, $dq0$ signals defined in respect to a local reference frame can be converted to a unified reference frame. Here we demonstrate this process using a photovoltaic inverter model based on [19]. The inverter is modeled by

$$\begin{aligned} \frac{d}{dt} v_b &= \frac{1}{v_b C_b} \left[P_{pv} - \frac{3}{2} (v_d \hat{i}_d + v_q \hat{i}_q) \right], \\ k &= K_p (v_b - v_{ref}) + K_i \int (v_b - v_{ref}), \\ \hat{i}_d &= k v_d, \hat{i}_q = k v_q, \hat{i}_0 = 0, \end{aligned}$$

where P_{pv} denotes the DC power at the output of the photovoltaic array, C_b is the bus capacitor (connected at the input of the switching devices), v_b is the bus capacitor voltage, and v_{ref} is the reference voltage for the bus capacitor control circuitry. The term $\frac{3}{2}(v_d \hat{i}_d + v_q \hat{i}_q)$ is the inverter output power in terms of $dq0$ signals. Based on [19], a simple PI controller is used here to control the bus voltage v_b . Hence, K_p and K_i denote the coefficients for the proportional and integral terms, respectively. The second part describes the inverter output capacitor as

$$\begin{aligned} \frac{d}{dt} \phi_1 &= \frac{1}{C_{sh}} (\hat{i}_d - i_d) + \omega_s \phi_2, \\ \frac{d}{dt} \phi_2 &= \frac{1}{C_{sh}} (\hat{i}_q - i_q) - \omega_s \phi_1, \\ \frac{d}{dt} \phi_3 &= \frac{1}{C_{sh}} (\hat{i}_0 - i_0) \end{aligned}$$

with $v_d = \phi_1$, $v_q = \phi_2$, $v_0 = \phi_3$, and where C_{sh} is the inverter output capacitance.

4. NUMERIC TEST CASES

This section shows several test cases that illustrate the main idea of modeling and analysis in the unified reference frame. Three networks with 4, 14, and 200 buses, whose parameters are taken from [15], are considered. The first example presents a brief comparison between the quasi-static, abc , and $dq0$ models. The second and third examples are devoted to the small-signal analysis of the 14- and 200-bus networks.

4.1. Comparison of quasi-static, abc , and $dq0$ models

Figure 3 illustrates comparison between conventional abc and $dq0$ models presented in terms of sparsity and total number of nonzero elements for various test-case networks taken from the MATPOWER database [15]. The sparsity indices are computed as the ratio between zero elements in all system matrices and the total number of elements. Observe that both models have approximately the same number of nonzero elements; however, the abc model is slightly sparser.

Consider now a simple 4-bus network. Its single-line diagram is shown in Fig. 4.

The quasi-static and $dq0$ models were constructed using the software package available in [16]. The abc model was implemented using MATLAB toolbox Simscape Power Systems. The transient behavior is analyzed under changing operating conditions as depicted in Fig. 5. The input voltage is subsequently changed from the initial value as follows. The ramp signal with the slope of 200 and upper limit of 10 kV is used to change the d component of the input voltage $v_{d,1}$ at time $t = 0.02$ s. Then the input is stepped from 10 to 20 kV at $t = 0.12$ s. The output current dq components are measured on bus 2. Observe that all models coincide in the steady state as expected. However, the abc and $dq0$ models are able to more accurately describe the transient behavior as they capture high-frequency phenomena.

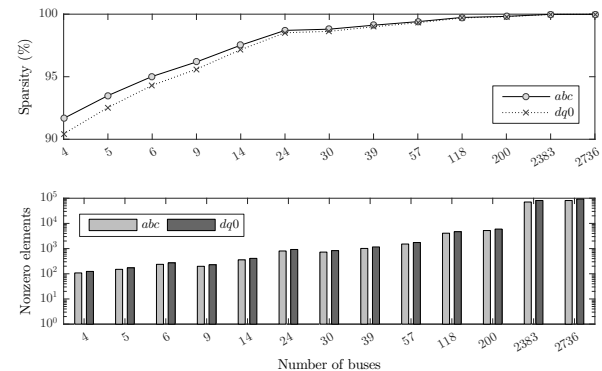


Fig. 3. Comparison between abc and $dq0$ models. The top plot presents the sparsity index, and the bottom plot illustrates the total number of nonzero elements.

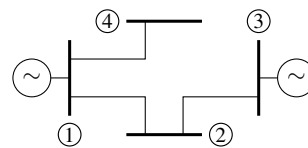


Fig. 4. Single-line diagram of a 4-bus system.

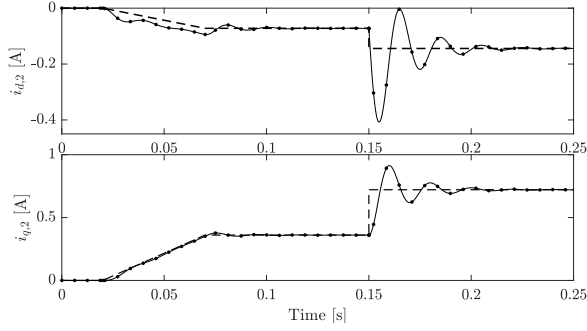


Fig. 5. Transient response of a 4-bus network. The lines correspond to quasi-static (- -), *abc* (—), and *dq0* (⋯⋯) models.

4.2. A 14-bus network

Consider now the IEEE 14-bus system. This network was modified by replacing synchronous machines connected to buses 6 and 8 by photovoltaic generators. Figure 6 shows a single-line diagram of the system, which is composed of two 300 and 150 MW synchronous generators and two 20 MW photovoltaic energy sources. In this figure, the values of P in MW and Q in MVar represent the operating point, which is obtained by solving the power flow equations. Bus 1 represents an infinite bus modeled by a voltage source. The complete system is constructed in the unified $dq0$ reference frame. A sketch of the signal flow diagram of the complete system is shown in Fig. 7.

Simulation parameters of synchronous machines are given in Table 2. Note that mechanical input powers ($P_m \approx T_m \omega_s$) are used as new external inputs.

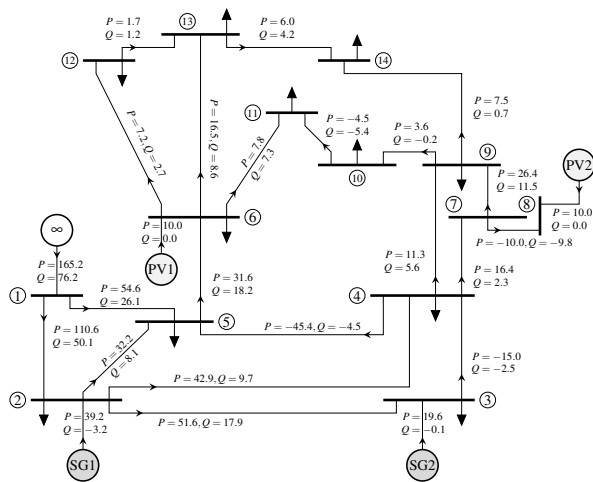


Fig. 6. Single-line diagram of a 14-bus system with two synchronous machines (SG) and two renewable energy sources (PV). Values of P and Q denote the operating point (power flow solution).

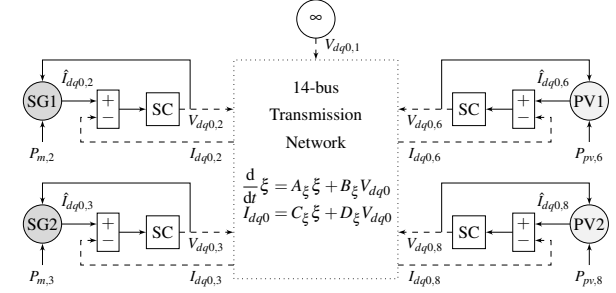


Fig. 7. Sketch of the signal flow diagram for the complete system. The following blocks are used: synchronous generator (SG), shunt capacitor (SC), photovoltaic generator (PV), and infinite bus (∞). Signals entering the network (dashed lines) are subject to rerouting.

Parameters of the infinite bus are $v_{d,1} = 1.5 \cdot 10^5$ V and $v_{q,1} = v_{0,1} = 0$ V. Moreover, $\omega_s = 2\pi 50$ rad/s is used to define the frequency of the unified reference frame. Simulation parameters for photovoltaic generators are given in Table 3.

Further we perform a small-signal stability analysis of an interconnected system, which is done in several steps: first the system's operating point is computed by solving the system power flow equations and converting the resulting complex voltages and currents to $dq0$ quantities. Next, unit models are linearized in the neighborhood of this operating point, and the overall system is described using state equations. We start with the nominal case and use the initial values provided in Tables 2 and 3. An array of Bode plots representing the frequency responses of the linear model is illustrated in Fig. 8 for $P_{m,2} \rightarrow P_2$ and $P_{m,3} \rightarrow P_2$ input-output pairs. These figures demonstrate that synchronous machines are weakly coupled at low frequencies but nonetheless affect each other at a certain resonance frequency of about 30 rad/s.

Table 2. Simulation parameters: synchronous machine

Parameter	SG1	SG2	Units
R_a	5.46	10.2	Ω
R_f	48.28	90.2	Ω
L_{ff}	57.93	108.24	H
L_{af}	2.46	4.59	H
J	$1.59 \cdot 10^3$	$0.79 \cdot 10^3$	kg.m ²
$L_d = L_q = 0.1L_0$	0.21	0.39	H
P_m	120	60	MW

Table 3. Simulation parameters: photovoltaic generator

Parameter	C_b	v_{ref}	C_{sh}	P_{pv}	K_p	K_i
PV1, PV2	60	800	3.18	30	$1.3 \cdot 10^{-6}$	0.3
Units	μF	V	μF	MW	-	-

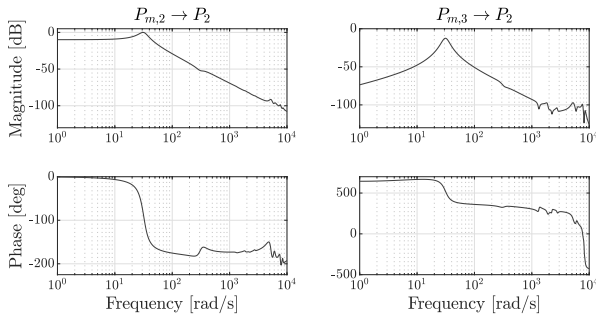


Fig. 8. Frequency responses in a 14-bus network.

In addition, as expected, high frequencies in the mechanical powers are filtered by the network inductances and synchronous machines inertia.

The transient process is shown in Fig. 9 for active powers. As expected, the infinite bus reacts to the changes in power generation. Table 4 provides numeric information for the largest eigenvalues. These results are then visualized in Fig. 10(a), which shows the root locus of dominant poles for 3 intervals of changing operating conditions. In addition, steps are depicted in Fig. 10(b).

Next, the dynamic behavior is analyzed under the changing operating conditions as presented in Fig. 10(b). The nonlinear models of units are then re-linearized in the neighborhood of new operating points when the transient process is complete and the system is in the steady state. Time instances are selected as $t \in \{1.9, 3.9, 5.9, 8\}$. Signals are subsequently changed from their initial values as follows. The mechanical powers $P_{m,2}$ and $P_{m,3}$ of SG1 and SG2 at buses 2 and 3 are increased from 120 to 180 MW at $t = 2$ s and from 60 to 90 MW at $t = 6$ s, respectively. The DC power $P_{pv,6}$ at the output of the photovoltaic array PV1 connected to bus 6 is decreased from 30 to 15 MW at $t = 4$ s, while $P_{pv,8}$ is kept constant (30 MW).

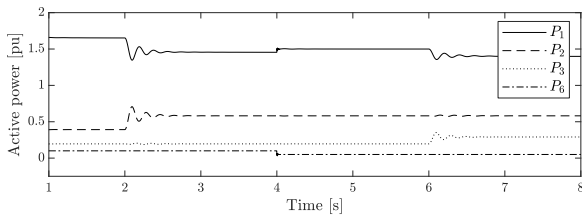
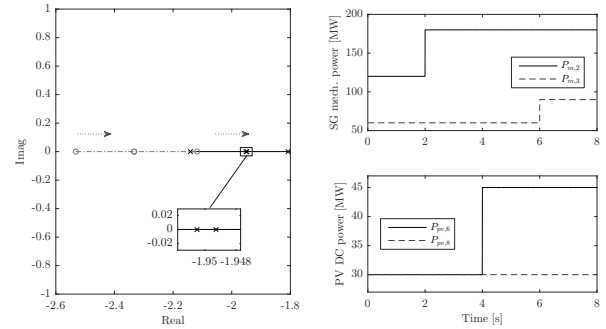


Fig. 9. Transient process of single-phase active powers.

Table 4. Change of the dominant eigenvalues

Eig. #	Initial	$P_{m,2}$	$P_{pv,6}$	$P_{m,3}$
1	-2.1397	-1.9505	-1.9493	-1.8084
2	-2.5316	-2.3335	-2.333	-2.1191



(a) Root locus of the eigen- (b) Change in $P_{m,2}$, $P_{m,3}$, $P_{pv,6}$ values

Fig. 10. Eigenanalysis: root locus of the dominant eigenvalues when external input signals are changed. Dotted arrows indicate the direction of poles change.

From Fig. 9 it can be seen that the provided changes in input powers directly affect the steady-state conditions and cause a change of the operating point. The presented analysis may assist in understanding the dynamic behavior of the system. For example, from Fig. 10(a) it follows that poles move toward the origin, which means that the response of the system becomes slower with the increase of external powers. In addition, observe that a change in the DC power $P_{pv,6}$ of the photovoltaic array connected to bus 6 has a minor effect (zoomed area in Fig. 10(a)) on the overall dynamics of the system, because poles are slightly moved from their positions. This is due to the fact that the photovoltaic inverter connected to the grid is less powerful than the respective synchronous machines. Clearly, if the amount or the overall capacity of photovoltaic energy sources is increased, the effect will be more significant. This, in particular, means that the proposed approach may help to estimate the amount of renewable energy produced by PVs within the stability limits.

4.3. A 200-bus network

In this section, we show that the proposed approach can be applied for the analysis of larger systems. In particular, consider a 200-bus system. A detailed description and numeric values can be found in [15] based on [20]. Models of the transmission network, generators, and loads are constructed using [21]. Generators are described using the swing equation (6), and loads are represented based on the balanced series RL impedances. The small-signal model is obtained similarly to the case of the 14-bus network. The complete (with attached units and loads) $dq0$ model has 1470 states and 48 external input signals (mechanical powers). All the components are modeled in the unified reference frame rotating with $\omega_s = 2\pi 50$ rad/s. The sparsity pattern of the matrix A (sparsity index is 0.49%) and the distribution of the dominant eigenvalues are shown in Fig. 11. The dynamic

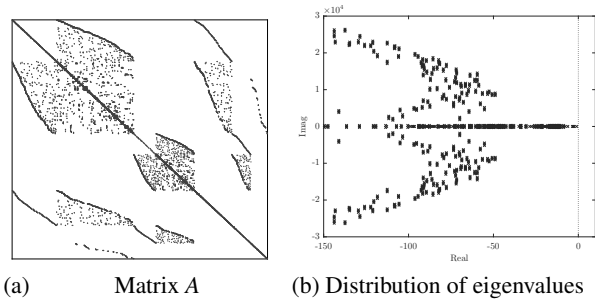


Fig. 11. Sparsity pattern of the matrix A and the distribution of the dominant eigenvalues for the $dq0$ model of the feedback-connected 200-bus system.

behavior is further analyzed under changing operating conditions to demonstrate similarities and differences between quasi-static and $dq0$ models.

Scenario (similarities): In the first test case the system is simulated under the nominal conditions, and then the overall active power demand of all loads is increased by 15% and 35% from 2229 to 2563 and 3009 MW, respectively. Table 5 provides numeric information, in which the first three eigenvalues with the largest real parts are shown for both quasi-static (qs) and $dq0$ models. Observe that both quasi-static and dq models provide almost identical dominant poles.

Scenario (differences): Consider first the case when the moment of inertia (J) of the synchronous machine connected to bus 196 is changed. The moment of inertia is first increased and then decreased by 4 times from the nominal value. The dominant poles of the quasi-static and dq models are similar for higher values but differ for a smaller moment of inertia. Table 6 provides numeric information, in which the first several eigenvalues with the largest real part are shown. Observe that the dq model predicts that the system is unstable, but the quasi-static model fails to predict this instability.

Consider now the case when several line resistances are changed. In particular, we change the branch resistances for the lines connecting buses $135 \rightarrow 133$, $136 \rightarrow 133$, and $189 \rightarrow 187$. First, branch resistances are increased by 1.5 times and then decreased by 5 times from their nominal values. Table 7 provides the numeric information, in which the first three eigenvalues with the

Table 5. Dominant poles: increase in active power consumption

Model	Eig. #	Nominal	Step (15%)	Step (35%)
$dq0$	1	-1.1751	-1.0612	-0.7555
qs		-1.1706	-1.0570	-0.7522
$dq0$	2	-2.6954	-2.6062	-2.3191
qs		-2.6896	-2.6007	-2.3174
$dq0$	3	-2.7720	-2.6549	-2.3553
qs		-2.7697	-2.6517	-2.3473

Table 6. Dominant poles: change in the moment of inertia

Model	Eig. #	Nominal	Increase	Decrease
$dq0$	1	-1.5044	-1.4843	$3.25 \pm 267.8j$
qs		-1.5019	-1.4819	-1.5064
$dq0$	2	-2.8441	-2.8422	
qs		-2.8447	-2.8407	-2.8455
$dq0$	3	-2.9222	-2.9204	-1.5100
qs		-2.9200	-2.9183	-2.9203

Table 7. Dominant poles: change in branch resistances

Model	Eig. #	Nominal	Increase	Decrease
$dq0$	1	-1.5044	-1.5031	$0.13 \pm 310.98j$
qs		-1.5019	-1.5006	-1.5040
$dq0$	2	-2.8441	-2.8471	
qs		-2.8447	-2.8437	-2.8463
$dq0$	3	-2.9222	-2.9209	-1.5100
qs		-2.9200	-2.9188	-2.9220

largest real part are shown. Observe that although the quasi-static model provides quite similar results for the ‘increase’ case, it fails to predict instability when resistances are decreased.

This example shows that the traditional small-signal stability analysis based on quasi-static approximation of the network has to be used carefully as in some cases it may give misleading results.

5. DISCUSSION AND CONCLUSIONS

A developing solution to model the dynamics of large-scale power systems is to use $dq0$ quantities, assuming that the transmission network is symmetrically configured. This approach combines two properties of interest: similar to transient models, $dq0$ -based models are derived from physical models and are therefore accurate at high frequencies. In addition, similarly to time-varying phasor models, $dq0$ models are time invariant. This property allows one to define an operating point and enables small-signal analysis. As a result, $dq0$ -based analysis is expected to be beneficial when considering the stability of large-scale power networks that include a variety of distributed and renewable power sources.

A current challenge is to merge various $dq0$ -based models appearing in the literature to obtain a complete model of a large power system. In this paper we approach this problem by representing various $dq0$ models in a reference frame rotating with a unified angle. This enables direct connections between units of different types and the network and provides a means to perform a small-signal stability analysis of large-scale systems. This approach is demonstrated on the basis of two standard units (synchronous machine and photovoltaic generator), and in addition, a model of the transmission network based on the unified reference frame is provided. The paper is

accompanied by a free software package available in [16] that constructs the proposed dynamic models and provides tools for dynamic simulations and stability studies based on $dq0$ quantities. Three particular examples are presented in this paper.

ACKNOWLEDGMENTS

J. Belikov was supported by the Estonian Research Council grant MOBTP36. Y. Levron was partly supported by the Grand Technion Energy Program (GTEP). The publication costs of this article were covered by the Estonian Academy of Sciences.

REFERENCES

- Ilić, M. and Zaborszky, J. *Dynamics and Control of Large Electric Power Systems*. Wiley, New York, 2000.
- Demiray, T. and Andersson, G. Comparison of the efficiency of dynamic phasor models derived from ABC and DQ0 reference frame in power system dynamic simulations. In *The 7th IET International Conference on Advances in Power System Control, Operation and Management*. Hong Kong, China, 2006, 1–8.
- Yang, T., Bozhko, S. V., and Asher, G. M. Modeling of uncontrolled rectifiers using dynamic phasors. In *Electrical System for Aircraft, Railway and Ship Propulsion (ESA RS)*. IEEE, 2012, 1–6.
- Fitzgerald, A. E., Kingsley, C., and Umans, S. D. *Electric Machinery*. McGraw-Hill, New York, 2003.
- Eid, A. Utility integration of PV-wind-fuel cell hybrid distributed generation systems under variable load demands. *Int. J. Elec. Power*, 2014, **62**, 689–699.
- Huang, B. and Handschin, E. Characteristics of the dynamics of distribution electrical networks. *Int. J. Elec. Power*, 2008, **30**(9), 547–552.
- Teodorescu, R., Liserre, M., and Rodriguez, P. *Grid Converters for Photovoltaic and Wind Power Systems*. John Wiley & Sons, 2011.
- Sauer, P. W., Lesieutre, B. C., and Pai, M. A. Transient algebraic circuits for power system dynamic modelling. *Int. J. Elec. Power*, 1993, **15**(5), 315–321.
- Krause, P. C., Wasynczuk, O., Sudhoff, S. D., and Pekarek, S. *Analysis of Electric Machinery and Drive Systems*. Wiley-IEEE Press, 2013.
- Schiffer, J., Zonetti, D., Ortega, R., Stanković, A. M., Sezi, T., and Raisch, J. A survey on modeling of microgrids—From fundamental physics to phasors and voltage sources. *Automatica*, 2016, **74**, 135–150.
- Katiraei, F., Iravani, M. R., and Lehn, P. W. Small-signal dynamic model of a micro-grid including conventional and electronically interfaced distributed resources. *IET Gener. Transm. Dis.*, 2007, **1**(3), 369–378.
- Levron, Y. and Belikov, J. Observable canonical forms of multi-machine power systems using dq0 signals. In *IEEE International Conference on the Science of Electrical Engineering*. Eilat, Israel, 2016, 1–6.
- Belikov, J. and Levron, Y. A sparse minimal-order dynamic model of power networks based on dq0 signals. *IEEE Trans. Power Syst.*, 2018, **33**(1), 1059–1067.
- Levron, Y. and Belikov, J. Modeling power networks using dynamic phasors in the dq0 reference frame. *Electr. Pow. Syst. Res.*, 2017, **144**, 233–242.
- Zimmerman, R. D., Murillo-Sánchez, C. E., and Thomas, R. J. MATPOWER: steady-state operations, planning, and analysis tools for power systems research and education. *IEEE Trans. Power Syst.*, 2011, **26**(1), 12–19.
- Levron, Y. and Belikov, J. DQ0 dynamics—Software manual. Technion—Israel Institute of Technology, Haifa, Israel, 2017. <https://a-lab.ee/sites/default/files/manual.pdf>.
- Sauer, P. W. and Pai, M. A. *Power System Dynamics and Stability*. Prentice Hall, Upper Saddle River, New Jersey, 1998.
- Szcześniak, P., Fedyczak, Z., and Klytta, M. Modelling and analysis of a matrix-reactance frequency converter based on buck-boost topology by DQ0 transformation. In *The 13th International Power Electronics and Motion Control Conference*. Poznan, Poland, 2008, 165–172.
- Levron, Y., Canaday, S., and Erickson, R. W. Bus voltage control with zero distortion and high bandwidth for single-phase solar inverters. *IEEE Trans. Power Electron.*, 2016, **31**(1), 258–269.
- Birchfield, A. B., Xu, T., Gegner, K. M., Shetye, K. S., and Overbye, T. J. Grid structural characteristics as validation criteria for synthetic networks. *IEEE Trans. Power Syst.*, 2017, **32**, 3258–3265.
- Levron, Y. and Belikov, J. Open-source software for modeling and analysis of power networks in the dq0 reference frame. In *IEEE PES PowerTech Conference*. Manchester, UK, 2017, 1–6.

Energiavõrkude dünaamiline modelleerimine ja stabiilsuse analüüs, kasutades $dq0$ teisendust ning ühtlustatud koordinaadisüsteemi

Juri Belikov ja Yoash Levron

$dq0$ koordinaadisüsteem on muutunud väga populaarseks traditsiooniliste masinate ja väikeste energiaallikate modelleerimiseks ning juhtimiseks. Kuid selle lai kasutus suuremõõtmeliste energiasüsteemide modelleerimiseks ja analüüsiks on ikka veel lahtine küsimus. Üheks tüüpiliseks $dq0$ mudeli probleemiks on lokaalsed koordinaadisüsteemid, mistõttu erinevate mudelite ühendamine pole alati otsene. Artiklis on välja pakutud lähenemine, kus võrk ja selle komponente on modelleeritud, kasutades $dq0$ teisendust, mis põhineb unifikseeritud koordinaadisüsteemil. See idee on illustreeritud, kasutades sünkroonsete masinate ja päikesegeneraatorite mudeleid. Kõik mudelid kasutavad unifikseeritud koordinaadisüsteemi, mistõttu need kõik saavad otseselt üksteisega ühenduda nii simulatsioonis kui ka analüütiliselt. Artikliga on kaasas tasuta tarkvarapakett, mis konstrueerib pakutud dünaamilised mudelid.